Available online at www.sciencedirect.com
ScienceDirect
Trans. Nonferrous Met. Soc. China 25(2015) 1575−1579
Transactions of Nonferrous Metals Society of China
www.tnmsc.cn

Preparation and properties of $Ni_{68.6}W_{17.9}B_{13.5}$ metallic glass

Jia-jia ZHANG, Wen-sheng LIU, Yun-zhu MA, Xiao-shan YE, Ya-yu WU, Bo-yun HUANG

State Key Laboratory of Powder Metallurgy, Central South University, Changsha 410083, China

Received 4 May 2014; accepted 1 September 2014

Abstract: A novel Ni-based metallic glass, i.e., $Ni_{68.6}W_{17.9}B_{13.5}$ (mole fraction, %), was prepared using melt spinning method. The results showed that the element B has much effect on the glass forming ability of the Ni−W−B metallic glass. Ni−W−B metallic glass could not be fabricated with lower content of B, whereas a higher content of 13.5% B could easily lead to the fully amorphous structure. The glass transition temperature and the onset temperature of crystallization are as high as 768 K and 781.5 K, respectively, and the crystallization activation energy calculated by Ozawa model is (637±60) kJ/mol, which showed strong thermal stability of $Ni_{68.6}W_{17.9}B_{13.5}$ metallic glass. This novel Ni-based metallic glass also exhibited good mechanical properties with the tensile strength of about 2331 MPa. The results indicate that this metallic glass should have a promising application in high strength material.
Key words: Ni-based metallic glass; activation energy; thermal stability; tensile strength

1 Introduction

Due to their high strength, strong thermal stability and good corrosion resistance, Ni-based metallic glasses are attracting increasing attention [1]. To date, many Ni-based metallic glasses with excellent properties have been reported [2−6]. However, most of the Ni-based metallic glasses are developed in the order of Ni−Zr [3], Ni−Nb [4], Ni−Ta [5] and Ni−Ti [6], other new system of the Ni-based metallic glasses has seldom been reported. On the other hand, Ni-based metallic glasses are metastable phase. The thermal stability of metallic glasses is determined by the crystallization temperature [7]. They will transform into crystalline alloys, when the applied temperature is higher than the crystallization temperature. Few of the Ni-based metallic glasses could be used at the temperature higher than 1000 K [2−6]. In order to be used in higher temperature fields, it is desirable to enhance the crystallization temperature of Ni-based metallic glasses. It is known that refractory elements such as Nb, Ta and W can improve the thermal stability of metallic glasses [8]. The W−Ru−B ternary metallic glass with high tungsten content was fabricated by OHTSUKI et al [9], they found that the crystallization temperature of this metallic glass was higher than 1000 K. Therefore, in this study, the new ternary Ni-based metallic glass, $Ni_{68.6}W_{17.9}B_{13.5}$ (mole fraction, %), was explored based on eutectic compositions and fabricated by melt spinning method for the first time. The thermal stability and mechanical properties were investigated. It was found that this metallic glass possessed higher crystallization kinetics and higher tensile strength up to about 2331 MPa.

2 Experimental

Based on the eutectic compositions of $Ni_{79.3}W_{20.7}$, $B_{27}W_{73}$ and $B_{43}W_{57}$ (mole fraction, %), the Ni−W−B ternary compositions as $Ni_{73.7}W_{19.2}B_{7.1}$ and $Ni_{68.6}W_{17.9}B_{13.5}$ (mole fraction, %) were selected, respectively. The alloy ingots of both compositions were prepared by arc melting a mixture of pure metals in a Ti-gettered purified argon atmosphere. In order to improve chemical homogeneity, the ingots were remelted three times. The melt-spun ribbons were prepared by remelting the ingot in a quartz tube and ejecting onto a Cu wheel rotated with the surface speed of 30 m/s.

The $Ni_{68.6}W_{17.9}B_{13.5}$ ribbons with the width of 2−4 mm and the thickness of 25−35 μm were cut into samples with the length of about 30 mm, and then fixed onto sample clamps. The uniaxial tests were carried out

Foundation item: Project (50774098) supported by the National Natural Science Foundation of China; Project (50721003) supported by Creative Research Group of the National Natural Science Foundation of China; Project (CX2013B054) supported by the Innovative Research Project for Postgraduates in Hunan Province, China
Corresponding author: Yun-zhu MA; Tel: +86-731-88877825; E-mail: zhuzipm@csu.edu.cn
DOI: 10.1016/S1003-6326(15)63760-8

on a mechanical testing machine (INSTRON−3369) at a strain rate of 0.05 mm/min. The areas of the specimens fracture during tensile testing were examined by a scanning electron microscope (SEM, FEI Nova Nano−230). The samples were performed for testing, and the one close to the average value was adopted for the curve of tensile stress−strain. The structure of the melt-spun ribbons was examined by X-ray diffraction (XRD, RIGAKU–3104). The thermal stability was investigated by differential scanning calorimeter (DSC) at different heating rates ranging from 10 to 40 K/min. The microstructure was examined by a transmission electron microscope (TEM, ZOEL−2100F).

3 Results and discussion

3.1 Structure analysis

In order to investigate the effect of B element on the glass forming ability of the Ni−W−B alloy, two kinds of ribbons $Ni_{73.7}W_{19.2}B_{7.1}$ and $Ni_{68.6}W_{17.9}B_{13.5}$ were prepared in this study. Figure 1 shows the XRD patterns and optical image of as-prepared $Ni_{73.7}W_{19.2}B_{7.1}$ and $Ni_{68.6}W_{17.9}B_{13.5}$ ribbons. It can be seen that there are crystalline peaks of $Ni_{17}W_3$ on the XRD pattern of the $Ni_{73.7}W_{19.2}B_{7.1}$. However, the XRD pattern of $Ni_{68.6}W_{17.9}B_{13.5}$ displays only broad diffraction maximum without any detectable sharp Bragg peaks. This shows the typical pattern of amorphous structure of $Ni_{68.6}W_{17.9}B_{13.5}$. Figure 1(b) shows the optical photo of $Ni_{68.6}W_{17.9}B_{13.5}$ ribbons, it can be seen that the ribbons do not break when they were bended to a certain angle. These results indicate that the $Ni_{68.6}W_{17.9}B_{13.5}$ ribbons have excellent ability of ductility and can be regarded as fully amorphous phase. To further investigate the structure of $Ni_{68.6}W_{17.9}B_{13.5}$ ribbons, TEM image and the selected area electronic diffraction pattern were preformed and shown in Fig. 2. Clearly, no crystals were detected, further confirming its fully amorphous structure. The results suggest that 13.5% B (mole fraction) can effectively suppress the precipitation of the crystalline of $Ni_{17}W_3$ and greatly improve the glass forming ability of Ni−W−B alloy.

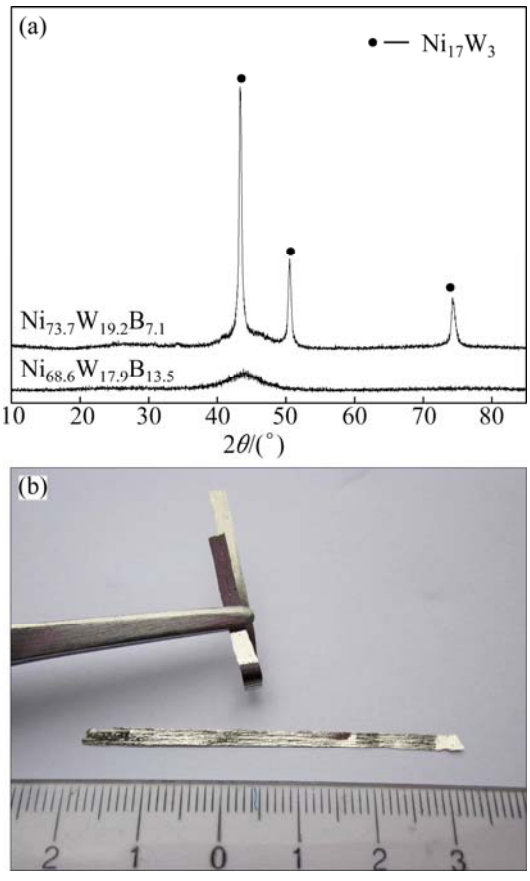

Fig. 1 XRD patterns of as-prepared $Ni_{73.7}W_{19.2}B_{7.1}$ and $Ni_{68.6}W_{17.9}B_{13.5}$ ribbons (a) and optical image of $Ni_{68.6}W_{17.9}B_{13.5}$ ribbons (b)

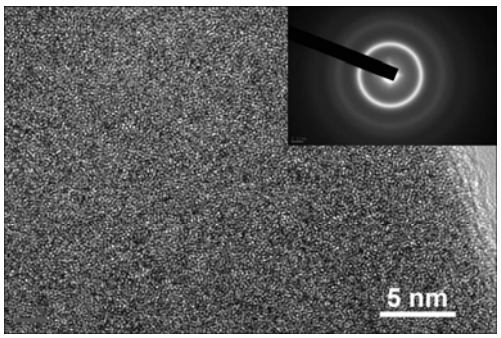

Fig. 2 TEM image of $Ni_{68.6}W_{17.9}B_{13.5}$ ribbon (Inset is selected area electronic diffraction pattern)

It should be noted that, in the $Ni_{68.6}W_{17.9}B_{13.5}$ amorphous ribbons, the atomic size decreases in the order of W (0.137 nm), Ni (0.125 nm) and B (0.079 nm), resulting in dense packing in liquid state. The elements of W and Ni can form the eutectic system with B, which is in agreement with the principles of eutectic [10]. In addition, the B element has large negative mixing enthalpy with the other constituent elements [11], implying strong cohesive forces among W, Ni and B atoms. Thus, the $Ni_{68.6}W_{17.9}B_{13.5}$ amorphous ribbons can be successfully prepared by melt spinning method.

3.2 Thermal stability

Figure 3 shows the DSC curve of the $Ni_{68.6}W_{17.9}B_{13.5}$ ribbons. It can be seen that the glass transition temperature (T_g) is 768 K, the onset temperature of crystallization (T_x) is 781.5 K, and the first exothermic peak temperature (T_p) is 794 K. In this study, due to the accuracy limit of DSC measurement in our experiment condition, we cannot detect the melt point of the $Ni_{68.6}W_{17.9}B_{13.5}$ amorphous ribbons, only the super-cooled liquid region ΔT (T_x-T_g)=13.5 K was obtained. However, the glass transition temperature T_g is as high as 768 K, which is higher than that of most other

metallic glasses, indicating a much higher thermal stability of this metallic glass.

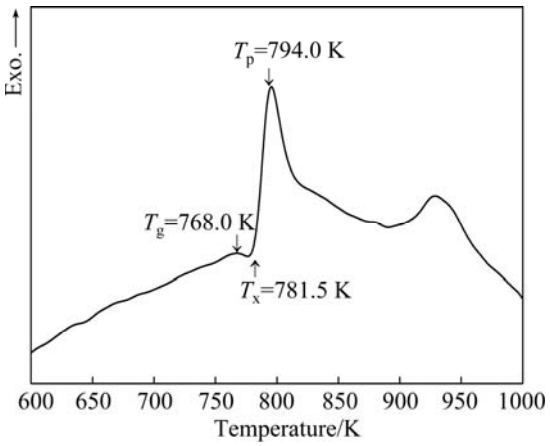

Fig. 3 DSC curve of $Ni_{68.6}W_{17.9}B_{13.5}$ amorphous ribbons

To investigate the thermal stability of the $Ni_{68.6}W_{17.9}B_{13.5}$ ribbons, the DSC curves obtained under different heating rates are shown in Fig. 4. It can be seen that with the increase of heating rate, the specific temperatures of T_x and T_p shift to high temperatures, and the exothermic peaks show an enhanced trend. The values of T_x and T_p are listed in Table 1. As the heating rate increases from 10 to 40 K/min, T_x increases from 781.5 to 792.5 K, and T_p raises from 794.0 to 803.0 K, which shows that the crystallization behavior of

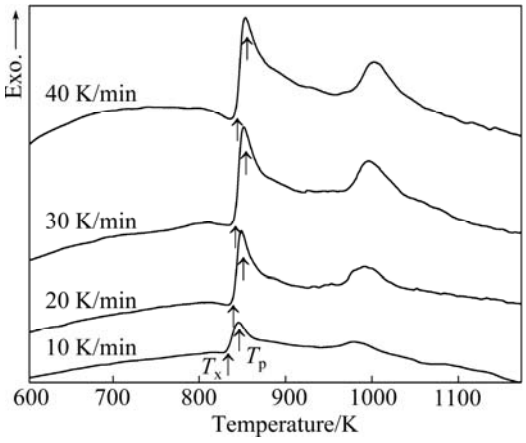

Fig. 4 DSC curves of $Ni_{68.6}W_{17.9}B_{13.5}$ amorphous ribbons under different heating rates

Table 1 T_x and T_p for $Ni_{68.6}W_{17.9}B_{13.5}$ amorphous ribbons at different heating rates

Heating rate/(K·min^{-1})	T_x/K	T_p/K
10	781.5	794.0
20	788.5	798.5
30	790.6	801.6
40	792.5	803.0

$Ni_{68.6}W_{17.9}B_{13.5}$ amorphous ribbons is closely associated with the heating rate.

In general, the specific temperatures of T_g and T_x can be simply assigned as the indicators of amorphous forming ability, but the crystallization activation energy (E) can reflect the energy barrier to overcome during crystallizing. The higher the crystallization activation energy is, the more stable the metallic glass will be. The crystallization activation energy can be evaluated by Kissinger equation and Ozawa equation, but due to the consideration of the changes of the specific temperature corresponding to the crystal fraction, the Ozawa equation is more consistent with the actual crystallization process, i.e. [12],

$$\ln b = -\frac{E}{R}\cdot\frac{1}{T} + C \quad (1)$$

where T stands for the specific temperature, b is the heating rate, E is the activation energy, R is the mole gas constant, and C is numeric constant. It can be seen from Eq. (1) that ln b versus $1/T$ yields to approximate straight lines with a slope of $-E/R$. Therefore, the activation energy of the $Ni_{68.6}W_{17.9}B_{13.5}$ amorphous ribbons can be obtained from the slope of lines. In this work, the T_x and T_p were adopted as the specific temperatures to calculate the activation energy of the $Ni_{68.6}W_{17.9}B_{13.5}$ amorphous ribbons. Figure 5 shows the Ozawa plots of the $Ni_{68.6}W_{17.9}B_{13.5}$ amorphous ribbons. It can be seen that the crystallization activation energy (E_x) is (637±60) kJ/mol, and the activation energy (E_p) is (798±31) kJ/mol. It should be noted that E_x is higher than those of Cu-based amorphous alloys (296 kJ/mol) [13], Zr-based amorphous alloys (402 kJ/mol) [14], Co-based amorphous alloys (452 kJ/mol) [15], Fe-based amorphous alloys (535 kJ/mol) [16], and so on. This further suggests the stronger thermal stability of the $Ni_{68.6}W_{17.9}B_{13.5}$ amorphous ribbons.

It is well known that the onset crystallization temperature is related to the grain nucleation process and

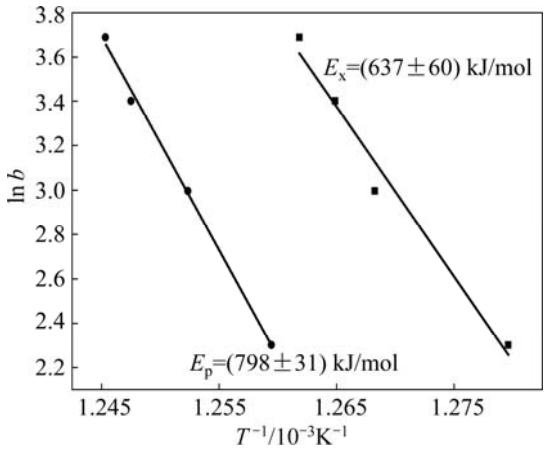

Fig. 5 Ozawa plot for $Ni_{68.6}W_{17.9}B_{13.5}$ amorphous ribbons

the peak temperature is associated with the grain growth process [17]. Thus, the activation energy E_x and E_p represent the activation energy for nucleation and growth, respectively. In Fig. 5, it can be seen that the activation energy E_p is about 150 kJ/mol higher than E_x, suggesting that grain growth is much slower than the nucleation process in the $Ni_{68.6}W_{17.9}B_{13.5}$ metallic glass. Thus, it can be inferred that the $Ni_{68.6}W_{17.9}B_{13.5}$ metallic glass may have an advantage of forming the composite materials with nanocrystallines and amorphous during certain annealing conditions [17].

3.3 Mechanical properties

In order to investigate the mechanical behavior of the $Ni_{68.6}W_{17.9}B_{13.5}$ ribbons, sample clamps were employed to fix the samples with the length of about 30 mm, and the uniaxial tensile tests were performed at a strain rate of 0.05 mm/min. The fracture cross section can be examined by SEM. Figure 6 shows the tensile stress−strain curve of the $Ni_{68.6}W_{17.9}B_{13.5}$ metallic glass. One can see that almost no plastic deformation occurs in the tensile stress−strain curve. When the elastic deformation reaches about 1.17%, catastrophic failure occurs. The tensile strength of the $Ni_{68.6}W_{17.9}B_{13.5}$ ribbon is about 2331 MPa, much higher than those of tungsten heavy alloys, whose tensile strength is usually 1000 MPa. However, the elastic deformation of the $Ni_{68.6}W_{17.9}B_{13.5}$ ribbon is not reliable, which may include the deformation of the sample clamps. The elastic deformation in Fig. 6 is not strictly linear, this is also because of the deformation of the sample clamps during tensile testing.

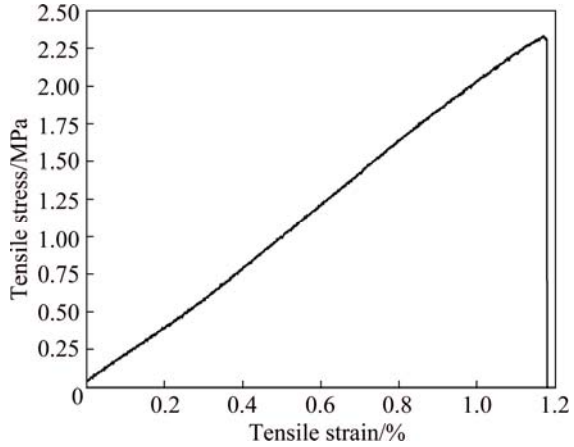

Fig. 6 Tensile stress−strain curve of $Ni_{68.6}W_{17.9}B_{13.5}$ amorphous ribbons

Figure 7 shows the SEM fracture microstructure of the $Ni_{68.6}W_{17.9}B_{13.5}$ ribbons. It can be observed that the venation pattern with the average diameter of about 2 μm distributes uniformly in the fracture. When catastrophic failure occurs, partial shear zones can be melted by the high energy, leading to the formation of venation pattern. It is interesting to find that a shear band fracture (as marked by arrow) with the width of about 4 μm is distributed at the edge of the sample fracture. This shows that the $Ni_{68.6}W_{17.9}B_{13.5}$ ribbon fractures along the shear band during the tensile test, and few shear bands are visible at the side perpendicular to the cross section, which suggests that the fracture process of $Ni_{68.6}W_{17.9}B_{13.5}$ ribbons is substantially dominated by a shear band. Because of the less shear bands, the overall fracture mode of the $Ni_{68.6}W_{17.9}B_{13.5}$ ribbon is brittle fracture without significant plastic deformation.

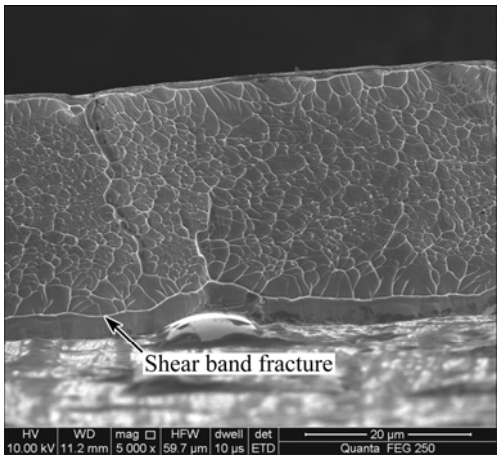

Fig. 7 SEM image of fracture of $Ni_{68.6}W_{17.9}B_{13.5}$ amorphous ribbons

4 Conclusions

1) The element B has effective effect on the glass forming ability of the Ni−W−B alloys. The Ni−W−B metallic glass could be fabricated by adding 13.5% B.

2) The crystallization activation energy simulated by Ozawa equation is (637±60) kJ/mol, suggesting a high thermal stability of $Ni_{68.6}W_{17.9}B_{13.5}$ metallic glass.

3) The tensile stress of $Ni_{68.6}W_{17.9}B_{13.5}$ metallic glass is about 2331 MPa. The fracture mode of $Ni_{68.6}W_{17.9}B_{13.5}$ amorphous ribbon is brittle fracture, and numerous venation patterns are observed to distribute uniformly on the fracture morphology.

References

[1] SURESH K, YSGESWARAN S, RAO K P, KOBAYSHI A, SHUM P W. Sliding wear behavior of gas tunnel type plasma sprayed Ni-based metallic glass composite coatings [J]. Vacuum, 2013, 88: 114−117.

[2] ZHANG T, INOUE A. New bulk glass Ni-based alloys with high strength of 3000 MPa [J]. Materials Transactions, 2002, 43(4): 708−711.

[3] XU Jing, ZHAO Zheng-feng, ZUO Min, XING Qi, SUN Zhe-xi, WANG Yan. Effects of Ca addition on the glass formation, microhardness and corrosion resistance in different solutions of $Zr_{66.7-x}Ni_{33.3}Ca_x$ (x=0, 1, 3 and 5 at.%) metallic glasses [J]. Journal of Alloys and Compounds, 2014, 595: 178−184.

[4] YU P, KIM K B, DAS J, BAIER F, XU W, ECKERT J. Fabrication

and mechanical properties of Ni−Nb metallic glass particle-reinforced Al-based metal matrix composite [J]. Scripta Materialia, 2006, 54: 1445−1450.

[5] TIEN H Y, LIN C Y, CHIN T S. New ternary Ni−Ta−Sn bulk metallic glasses [J]. Intermetallics, 2006, 14: 1075−7078.

[6] ZHU Zhen-dong, JIA Peng, XU Jian. Optimization for toughness in metalloid-free Ni-based bulk metallic glass [J]. Scripta Materialia, 2011, 64: 785−788.

[7] QIANG J B, ZHANG W, INOUE A. Ni−(Zr/Hf)−(Nb/Ta)−Al bulk metallic glasses with high thermal stabilities [J]. Intermetallics, 2009, 17: 249−252.

[8] DOLAN M D, HARA S, DAVE N C, HARAYA K, ISHITSCUKA M, ILYUSHECHKINA Y, KITA K, MCLENMAN K G, MORPETH L D, MUKAIDA M. Thermal stability, glass-forming ability and hydrogen permeability of amorphous $Ni_{64}Zr_{36-x}M_x$ (M=Ti, Nb, Mo, Hf, Ta or W) membranes [J]. Separation and Purification Technology, 2009, 65: 298−304.

[9] OHTSUKI M, TAMURA R, TAKEUCHI S. Hard metallic glass of tungsten-based alloy [J]. Applied Physics Letters, 2004, 14: 4911−4913.

[10] DONALD I W, DAVIES H A. Prediction of glass-forming ability for metallic systems [J]. Journal of Non-Crystalline Solids, 1978, 30(1): 77−85.

[11] BINNEWIES M, MIKE E. Thermochemical data of elements and compounds [M]. Weinhim: Wiley-VCH, 2002.

[12] OZAWA T. Kinetic analysis of derivative curves in thermal analysis [J]. J Therm Anal, 1970, 2(3): 301−324.

[13] YANG Y J, XING D W, CHEN J, SUN J F, WEI S D, HE H J, MECARTNEY D G. Crystallization kinetics of a bulk amorphous Cu−Ti−Zr−Ni alloy investigated by differential scanning calorimetry [J]. Journal of Alloys and Compounds, 2006, 415: 106−110.

[14] YAN Z J, HE S R, LI J R, ZHOU Y H. On the crystallization kinetics of $Zr_{60}Al_{15}Ni_{25}$ amorphous alloy [J]. Journal of Alloys and Compounds, 2004, 368: 175−179.

[15] YUAN Zi-zhou, CHEN Xue-ding, WANG Bin-xia, CHEN Zi-jiang. Crystallization kinetics of melt-spun $Co_{43}Fe_{20}Ta_{5.5}B_{31.5}$ amorphous alloy [J]. Journal of Alloys and Compounds, 2005, 399: 166−172.

[16] BISWAS K, RAM S, SCHULTZ L, ECKERT J. Crystallization kinetics of amorphous $Fe_{67}Co_{9.5}Nb_3Dy_{0.5}B_{20}$ [J]. Journal of Alloys and Compounds, 2005, 397: 104−109.

[17] WEI Heng-dou, CHEN Xue-ding, HAO Lei, ZHANG Jing. Non-isothermal crystallization and kinetics of $(Ni_{0.75}Fe_{0.25})_{78}Si_{10}B_{12}$ amorphous alloy [J]. Rare Metal Materials and Engineering, 2006, 35(11): 1720−1724.

$Ni_{68.6}W_{17.9}B_{13.5}$非晶合金的制备及性能

张佳佳，刘文胜，马运柱，叶晓珊，吴亚瑜，黄伯云

中南大学 粉末冶金国家重点实验室，长沙 410083

摘 要：采用单辊真空甩带法制备一种新型 Ni 基非晶合金($Ni_{68.6}W_{17.9}B_{13.5}$，摩尔分数)。结果表明：B 元素含量对 Ni−W−B 体系形成非晶合金具有较大影响，B 含量较低时不利于形成非晶合金，而当 B 含量高达 13.5% (摩尔分数)时可形成 Ni−W−B 非晶合金；$Ni_{68.6}W_{17.9}B_{13.5}$ 非晶合金的玻璃转化温度和晶化温度分别高达 768 K 和 781.5 K，采用 Ozawa 法计算其晶化激活能为(637±60) kJ/mol，表明其具有较高的热稳定性；$Ni_{68.6}W_{17.9}B_{13.5}$ 非晶合金的抗拉强度约为 2331 MPa，表明其具有在高强度领域应用的潜力。

关键词：镍基非晶合金；激活能；热稳定性；拉伸强度

(Edited by Xiang-qun LI)